



## **Mechanical Engineering Department**

Fall 2020

MENG 355 - Mechanics of Materials

### **Project 1 - Cykler's Right Leg Model**

Mohammed Taha

UID: 900183180

Instructor: Dr. Khalil Elkhodary

TA: Eng. Mohamed Atef

November 15, 2020

## Table of Contents

Table of Contents	1
List of Figures	2
Nomenclature	3
Abstract	4
Introduction	5
Assumptions	6
Calculations	7
Results	13
Conclusion and Reflection	17
Works Cited	20
Appendices	21

### **List of Figures**

- Figure 1: Free body diagram for foot
- Figure 2: Horizontal pedal force
- Figure 3: Vertical pedal force
- Figure 4: Joint Angles with crank angle
- Figure 5: Pedal angle with crank angle
- Figure 6: Leg parts' free body diagrams
- Figure 7: Bending moment diagrams for each part
- Figure 8: Maximum Normal  $\sigma$  Stress with Crank Angle
- Figure 9: Maximum Shear Stress  $\tau$  with Crank Angle
- Figure 10: Reaction at Joints with respect to Crank Angle
- Figure 11: Bending Moment at Joints with respect to Crank Angle
- Figure 12: Mohr Circle for Maximum Stress in Foot
- Figure 13: Mohr Circle for Maximum Stress in Shank
- Figure 14: Mohr Circle for Maximum Stress in Hip
- Figure 15: Angle Sketch
- Figure 16: Foot cross-section
- Figure 17: Femur cross-section
- Figure 18: Shank cross-section
- Figure 19: Skeleton Model
- Figure 20: Equivalent mechanical setup, pedal force graphs and angle graphs

## Nomenclature

Symbol	Description	Units
F	Force	kg.m/s <sup>2</sup> (Newtons N)
m	Mass	kg
g	Gravitational Acceleration	m/s <sup>2</sup>
P	Pressure	kN/m <sup>2</sup> (Pascale Pa)
A	Area	m <sup>2</sup>
V	Vertical shear force	kg.m/s <sup>2</sup> (Newtons N)
H	Horizontal shear force	kg.m/s <sup>2</sup> (Newtons N)
I	Second moment of Inertia	m <sup>4</sup>
$\theta$	Crank angle	° (Degrees)
$\beta$	Pedal angle	° (Degrees)
$\gamma$	Hip angle	° (Degrees)
$\Omega$	Knee angle	° (Degrees)
$\psi$	Ankle angle	° (Degrees)

## Abstract

**Background:** The human leg consists of 5 bone components: The femur, just below the hip. Patella (the knee), a joint lying below the femur joining it and the tibia and fibula (two parts comprising the leg shank), and the foot at the bottom. The biker pedals with two legs each situated on a crank on opposite sides of the bike which rotate the bike chain that operates the mechanism spinning the wheels and moving the bicycle.

**Objective:** Investigate the stresses generated near an average male body's leg bones and bones' joints while maintaining a constant speed on a typical road bike.

**Methods:** A detailed model of a skeleton is studied in the CAD program, SOLIDWORKS to use the ratios between the foot and bodily proportions to form an accurate as possible free body diagram to study the shear forces occurring in the tissue. Previous assessments have provided figures which relate the forces exerted to the angles produced by the leg between the crank and vertical axis (crank angle  $\theta$ ), and the angle between the horizontal axis and the foot (pedal angle  $\beta$ ). Average male bone dimensions, and body segment masses were used based mostly on various academic external sources available online. Some cross-sections were approximated from their natural complex shapes to more basic geometric shapes for a simpler analysis.

**Conclusion:** The shank was found to experience the greatest stress amongst the three parts of the leg. It experiences a maximum shear stress of about 16 MPa. The thigh would feel the second most shear stress at about 4 MPa. While the foot feels the least shear stress, 37 Kpa.

## Introduction

Human anatomy is an example of very complex and magnificent mechanical structural systems present in nature. Having an endoskeleton benefits a lot in allowing faster and more precise movement at the cost of being less flexible than hydrostatic skeleton creatures. A human bone can withstand a considerable amount of pressure before failing; having a tensile strength of about 150 MPa (Hazenbergh 2010). When designing a bicycle, ergonomics is taken into utmost consideration. There are standards dictating what strains the legs should overcome to uphold certain speeds, where skeletal structures of people of different age groups, ethnicities and gender are taken into consideration to portion the standard bike dimensions. This report documents our method of attempting to investigate the stresses in an average male body's **leg bones** while maintaining a constant speed on a typical road bike on a flat, horizontal surface.

### Assumptions

As a basis for our calculations, the following assumptions were made:

1. Mass of average male: 89.63 kg
2. Mass of thigh: 9.411 kg
3. Mass of foot: 1.2817 kg
4. Mass of shank: 5.54 kg
5. Foot length: 0.273 m
6. Shank length: 0.51051 m
7. Femur length: 0.52961 m
8. The femur has a cylindrical shape with a radius  $r=0.031395$  m
9. The foot has a rectangular cross-section with a width  $w=0.04914$  m and a height  $h=0.07098$  m
10. The shank has a cylindrical shape with a radius  $r=0.039585$  m
11. Part weights act on the middle of each part
12. Bones have a tensile strength of 150 MPa

(Gill, 2018., Plagenhoef, 2013)

## Calculations

Three critical sections, a-a, b-b, c-c will be taken on the leg, one just before each joint in each part of the leg. As afore mentioned, these calculations are aimed to examine the maximum stresses in the material of interest (bone), and reaction forces and reaction moments at each joint. It is predicted that the ultimate maximum stress would be around a tenth of the yield stress of bone, since a cyclist would never come close to fracturing their bones unless they were exposed to a sudden violent external force, or has severe bone deformations. This paper does not account for such abnormalities.

Symbol	Description	Unit
$\theta$	Crank angle	$^{\circ}$ (Degrees)
$\beta$	Pedal angle	$^{\circ}$ (Degrees)
$\gamma$	Hip angle	$^{\circ}$ (Degrees)
$\Omega$	Knee angle	$^{\circ}$ (Degrees)
$\psi$	Ankle angle	$^{\circ}$ (Degrees)

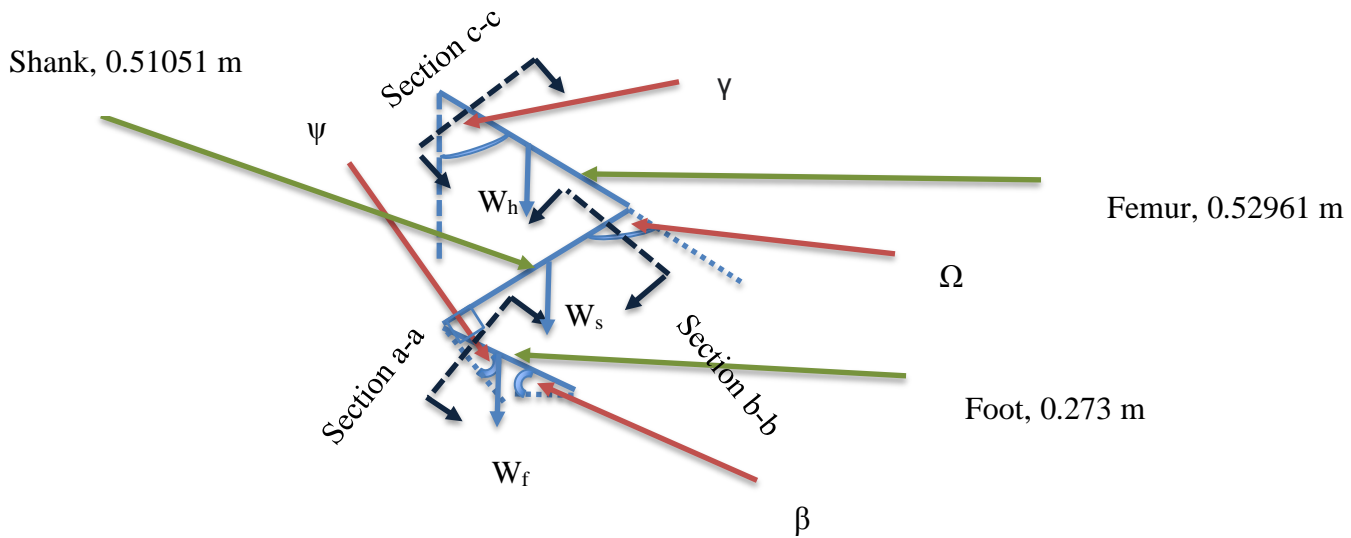


Figure 1: Free body diagram for foot



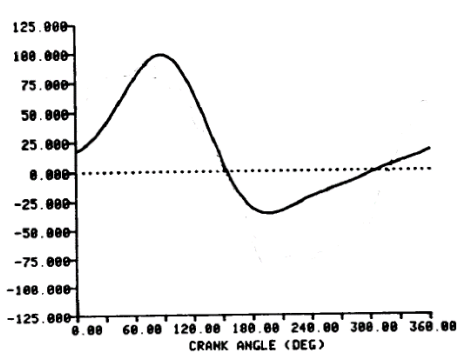


Figure 2: Horizontal pedal force

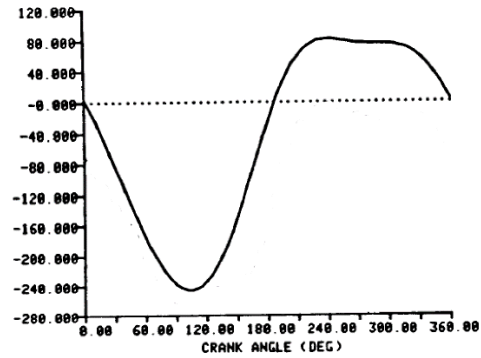


Figure 3: Vertical pedal force

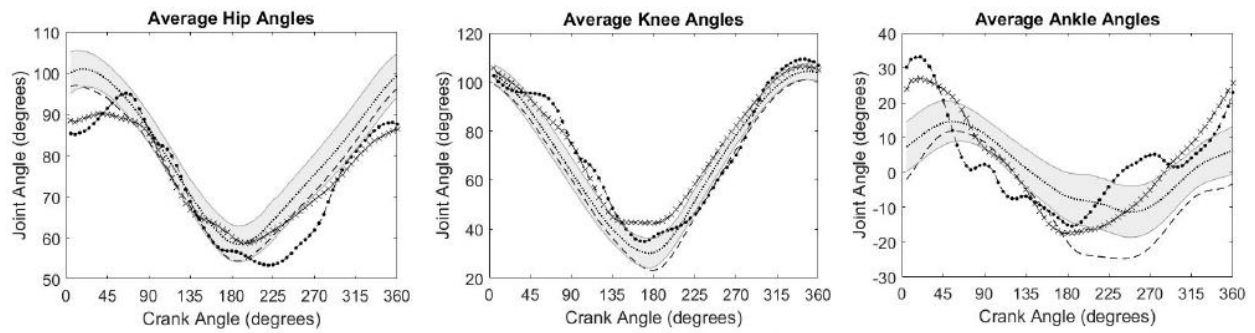


Figure 4: Joint Angles with crank angle

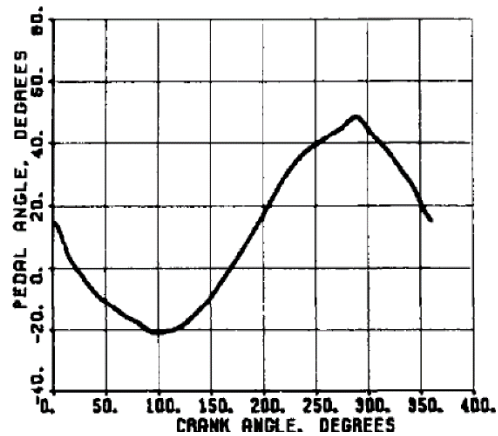


Figure 5: Pedal angle with crank angle

Crank Angle (degrees)	Horizontal Force (N)	Vertical Force (N)	Hip Angle (degrees)	Knee Angle (degrees)	Ankle Angle (degrees)	Pedal Angle (degrees)
0	18	0	91	102	6	15
5	20	-9	91	101	8	12
10	23	-21	92	99	9	8
15	28	-37	93	97	10	3
20	31	-58	93	95	11	0
25	36	-75	93	94	12	-2
30	42	-88	92	91	13	-4
35	49	-107	91	88	13	-6
40	55	-123	90	85	14	-8
45	64	-141	89	82	14	-9
50	70	-156	87	79	14	-11
55	76	-170	85	75	15	-12
60	82	-186	82	72	15	-13
65	89	-197	80	69	15	-14
70	93	-209	77	65	14	-15
75	97	-220	75	62	14	-17
80	99	-231	72	59	13	-18
85	99	-240	69	56	13	-18
90	99	-245	66	52	12	-19
95	98	-247	63	49	10	-20
100	95	-248	60	46	9	-20
105	91	-248	57	42	8	-20
110	85	-245	54	39	7	-20
115	77	-241	51	36	6	-20
120	69	-236	48	32	5	-19
125	58	-229	44	29	4	-17
130	49	-217	41	26	3	-16
135	37	-204	38	23	2	-14
140	26	-185	34	20	1	-12
145	15	-165	31	19	0	-11
150	5	-148	29	17	-2	-8
155	-4	-127	26	16	-3	-6
160	-12	-106	24	14	-3	-3
165	-18	-84	22	13	-4	-1
170	-23	-65	19	11	-5	2
175	-28	-42	18	11	-6	4
180	-31	-27	16	12	-7	7
185	-33	-11	16	13	-7	9
190	-35	13	15	14	-8	12
195	-35	26	15	16	-8	15

200	-36	38	15	19	-8	18
205	-35	50	17	21	-8	20
210	-34	60	18	25	-8	23
215	-32	68	20	30	-9	26
220	-30	72	22	33	-9	30
225	-29	77	24	37	-9	32
230	-28	80	27	41	-10	35
235	-25	83	30	46	-10	36
240	-23	83	33	49	-11	38
245	-21	83	35	52	-11	40
250	-19	82	37	55	-11	41
255	-18	81	38	59	-11	42
260	-17	81	41	62	-11	43
265	-15	81	44	66	-11	44
270	-13	81	46	69	-10	45
275	-10	79	48	72	-10	46
280	-9	78	50	76	-9	47
285	-7	76	52	80	-8	48
290	-5	76	55	83	-6	49
295	-3	76	58	86	-5	47
300	-2	76	61	89	-4	45
305	0	73	63	91	-3	43
310	2	71	65	93	-2	42
315	3	70	67	94	0	40
320	4	67	70	96	1	37
325	6	63	73	97	2	35
330	8	58	76	99	3	32
335	10	51	79	100	4	30
340	11	45	82	100	4	27
345	12	34	85	101	5	25
350	13	24	87	102	5	22
355	15	13	89	102	6	19
360	17	1	90	102	6	17

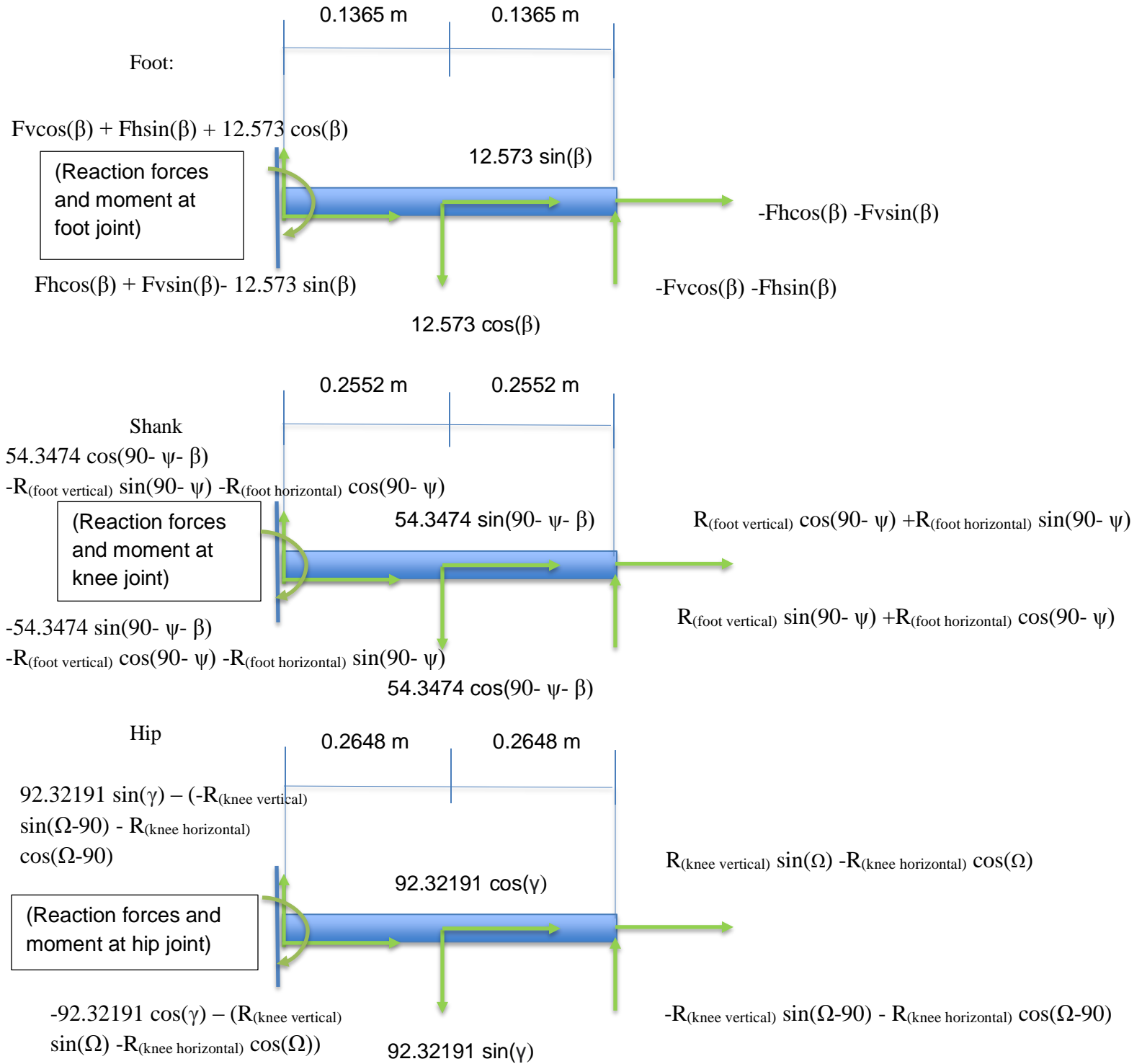


Figure 6: Leg parts' free body diagrams

Bending Moment Diagrams:

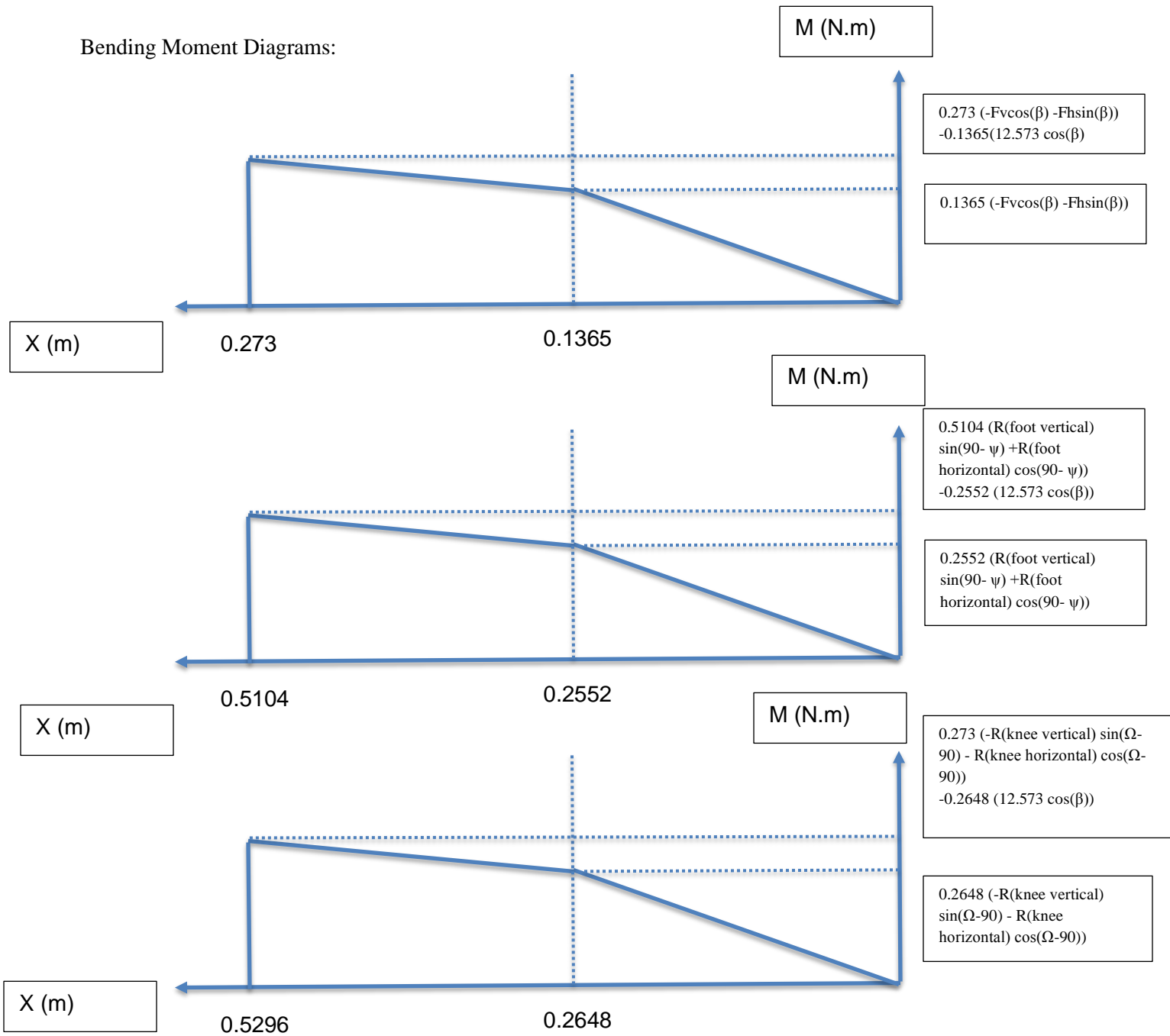


Figure 7: Bending moment diagrams for each part

## Results

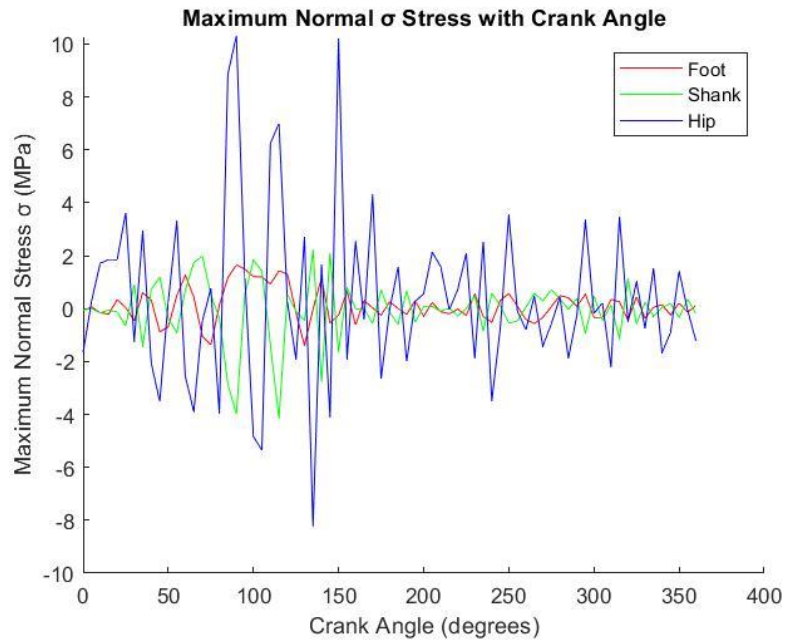


Figure 8: Maximum Normal  $\sigma$  Stress with Crank Angle

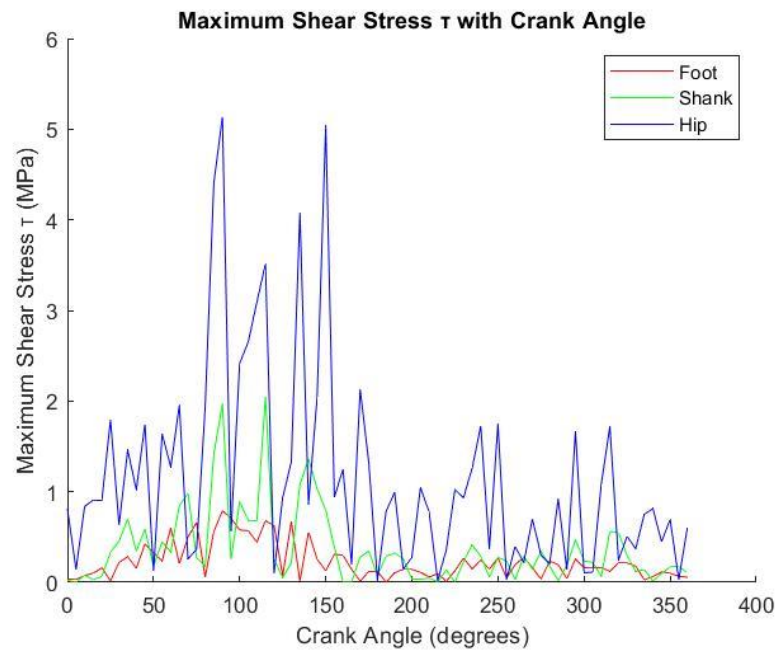


Figure 9: Maximum Shear Stress  $\tau$  with Crank Angle

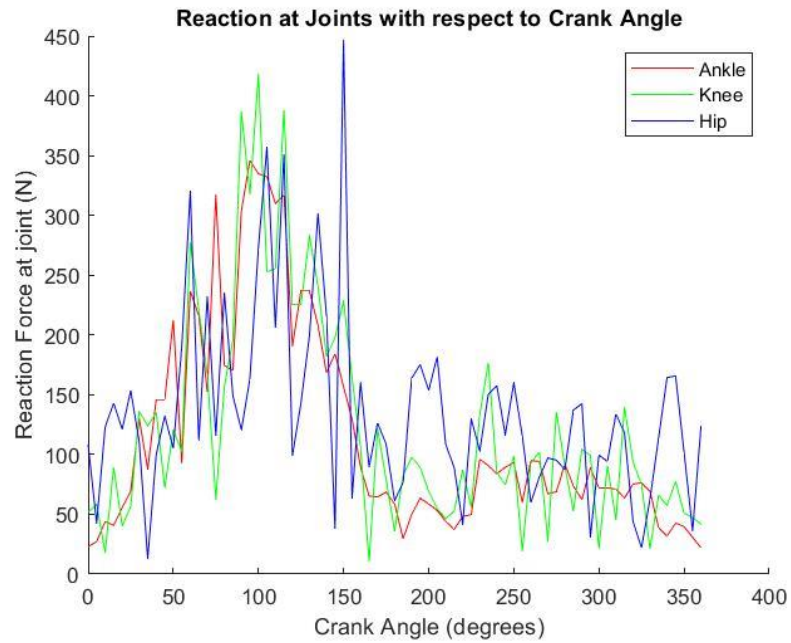


Figure 10: Reaction at Joints with respect to Crank Angle

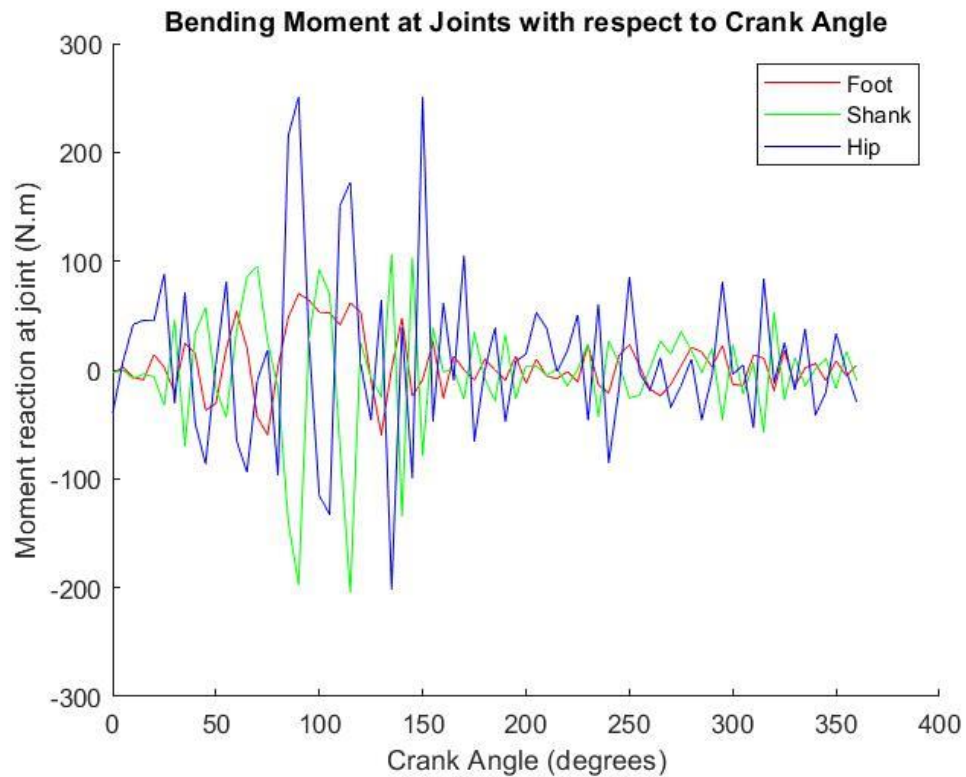
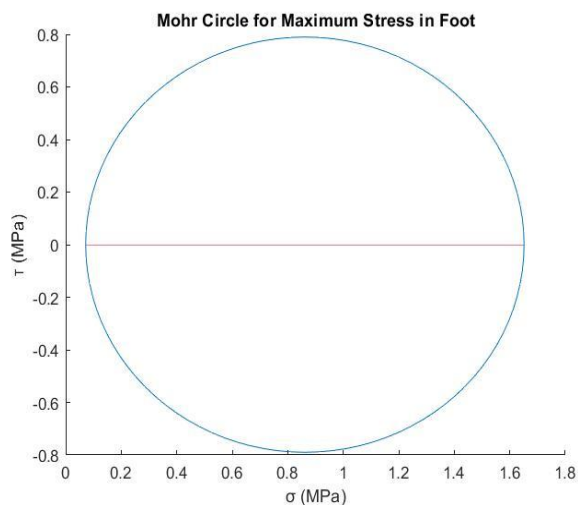


Figure 11: Bending Moment at Joints with respect to Crank Angle

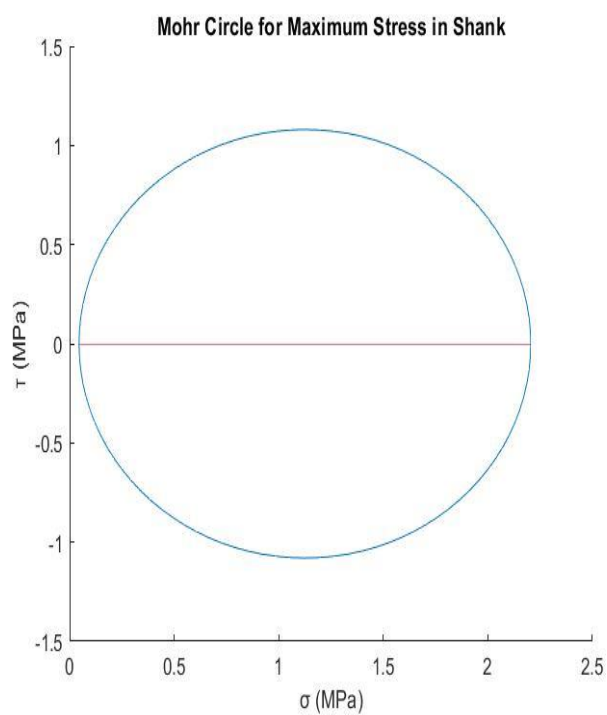


Stress Matrices (Foot) (MPa)

1.6516	0
0	0.071969

0.86176	-0.78979
0.78979	0.86176

Figure 12: Mohr Circle for Maximum Stress in Foot



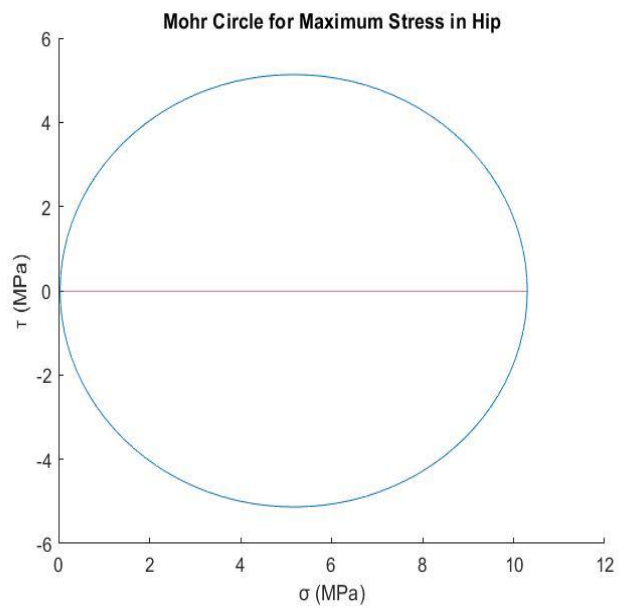
Stress Matrices (Shank) (MPa)

2.2050	0
0	0.045038

1.1250	-1.0800
1.0800	1.1250

Figure 13: Mohr Circle for Maximum Stress in Shank





Stress Matrices (Hip) (MPa)

10.301	0
0	0.034978

5.1679	-5.1329
5.1329	5.1679

Figure 14: Mohr Circle for Maximum Stress in Hip

## Conclusion and Reflection

The hip usually feels the most stress while cycling, much more than the shank and foot judging by the results obtained. The shank and foot interchange the largest stress along the crank cycle, but generally the shank would feel a minorly greater stress than in the foot. This ranking should be the result of the carry-over of the forces and moments through the leg parts from foot to hip.

The model reflects the real system to a limited degree due to the neglect of the intricate geometries of the real body parts, but it more or less depicts the stresses and reactions in a real human bone through a reasonable approximation which should nonetheless be close to the real ones, since the geometries may be an over-simplification, but not very deviating from the real.

The table of angles and forces were extracted from a few sources via a virtual graph data extraction tool which gave 73 points of data depending on the crank angles ranging from 0 to 360 degrees from the vertical axis. Minor errors might be a byproduct of using this, as data is not available to use directly, but rather taken graphically which would result in minor errors in taking the exact values of angles/forces. Also, the graphs only depict average relations of crank angles and forces/joint angles, so stresses would differ from a person to another with each experimentation. Overall, the accuracy and coverage of the crank angle cycle should be within norms of computational accuracy.

To verify the MATLAB code, at least two calculations at different crank angles were tested to verify the constancy of the computational results.

The stresses in the bones might differ based on the model parameters. A cyclist with a larger body-mass ratio would feel larger stresses in the leg bones as the weight would contribute a more significant portion of the reactions of the leg joints. A shorter person would have to experience a larger range of joint angles if the same model bicycle is used, vice versa for taller people with greater leg part parameters. Moments would contribute a greater portion in the taller person's foot stresses, hence feeling a greater stress in the bones than in shorter people.

The five-bar linkage model fit for this analysis is a suitable method of analyzing joint injury. The model would suggest injuries would occur close to joint areas as a result of the greatest build up of moment appearing there. A three-dimensional model is not necessary when analyzing a model of a cyclist mostly travelling in a uniform direction forward. For more violent cycling methods such as mountain biking where spontaneous forces from travelling on bumpy and inclined terrain while drifting left and right along a third axis is normal, a more detailed model which includes more information of the dynamics in those directions are provided would help better analyze where mountain biking injuries occur for such an instance.

If the rider in the model would be travelling up an incline, the forces acted on the pedal would vary significantly since the rider is combatting the friction with the ground induced by the bicycle and the rider's weights, while also driving against the force induced by the rider and bicycle's weights themselves at an inclination. In resolving the computational calculations, given the new forces directing the crank movement, the angles resolving the weight factor on the free body diagrams would remain the same, but the angle of inclination would be summed along them. For example, the vertical component of the weight acting on the hip component on the leg was calculated to be  $92.32191 \cdot \sin(\gamma)$ . Instead, it would become  $92.32191 \cdot \sin(\gamma + \text{angle of inclination})$ .

It would be expected that the shank would feel the most stress when assessing a model of a cyclist travelling up an incline, since the part would feel a great compressive force from both ends, the foot and hip throughout the cycle, while the weight of the foot and hip help alleviate some of the joint reactions from other members. Hence, in this instance the hypothesis would be that the shank would feel the greatest stress, followed by the foot then, lastly the hip.

### Works Cited

Beer, F. P. (2009). *Mechanics of materials*. New York: McGraw-Hill Higher Education.

Hazenber, Jan G. “Why Are Your Bones Not Made of Steel?” *Materials Today*, Materials Today, 22 Mar. 2010, [www.materialstoday.com](http://www.materialstoday.com).

Miroslav, Dařena. “Free CAD Designs, Files & 3D Models: The GrabCAD Community Library.” *Free CAD Designs, Files & 3D Models / The GrabCAD Community Library*, 19 May 2014, [grabcad.com/library/human-skeleton-1](http://grabcad.com/library/human-skeleton-1).

Gill, Stephan. “What Is the Average Weight for Men?” Edited by Judith Marcin, *Medical News Today*, MediLexicon International, 14 Feb. 2018, [www.medicalnewstoday.com/articles/320917](http://www.medicalnewstoday.com/articles/320917).

Plagenhoef, Stanley & Evans, F. & Abdelnour, Thomas. (2013). *Anatomical Data for Analyzing Human Motion*. *Research Quarterly for Exercise and Sport*. 54. 169-178.  
10.1080/02701367.1983.10605290.

## Appendices

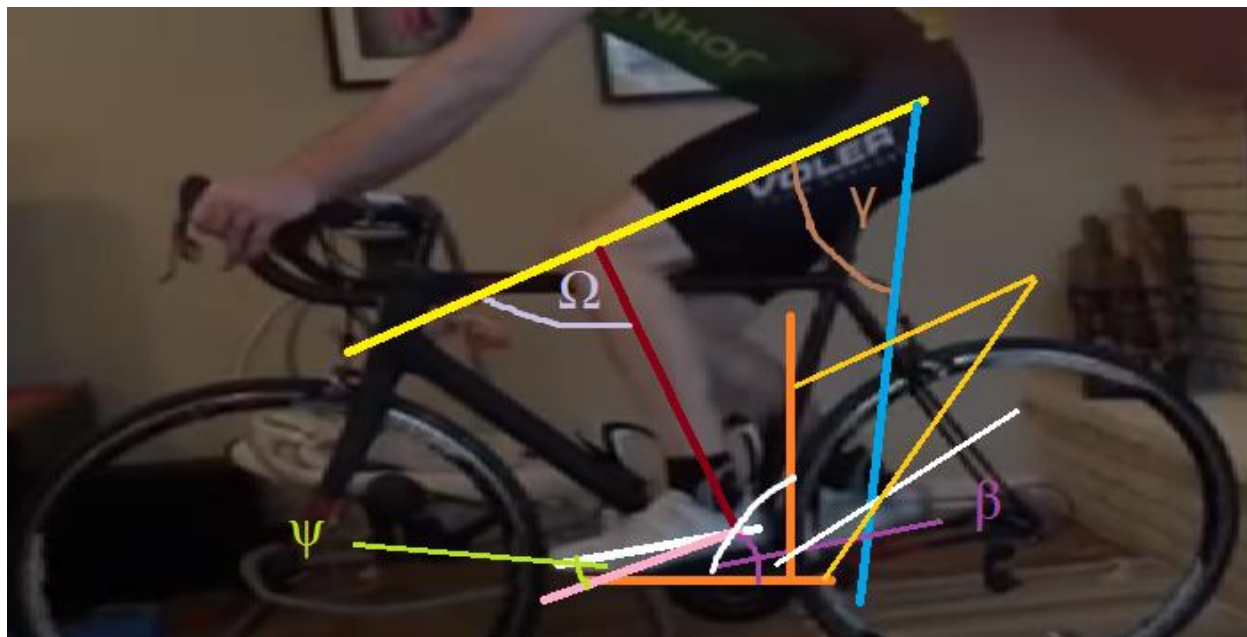


Figure 15: Angle Sketch

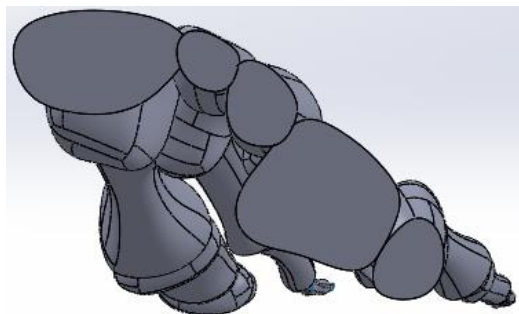


Figure 16: Foot cross-section

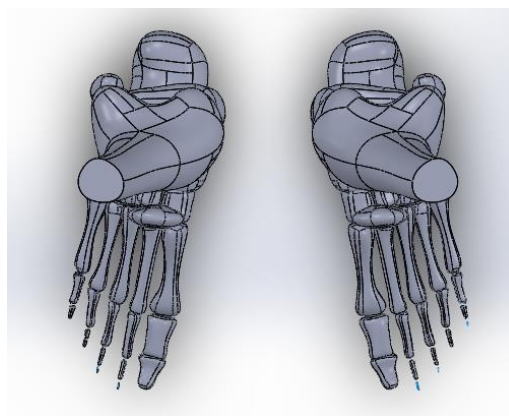


Figure 17: Femur cross-section

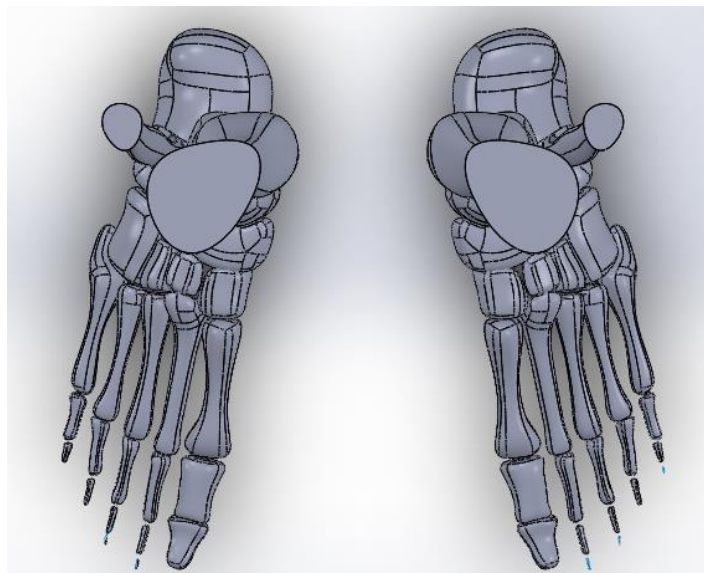


Figure 18: Shank cross-section

(Miroslav, 2014)



Figure 19: Skeleton Model

(Miroslav, 2014)

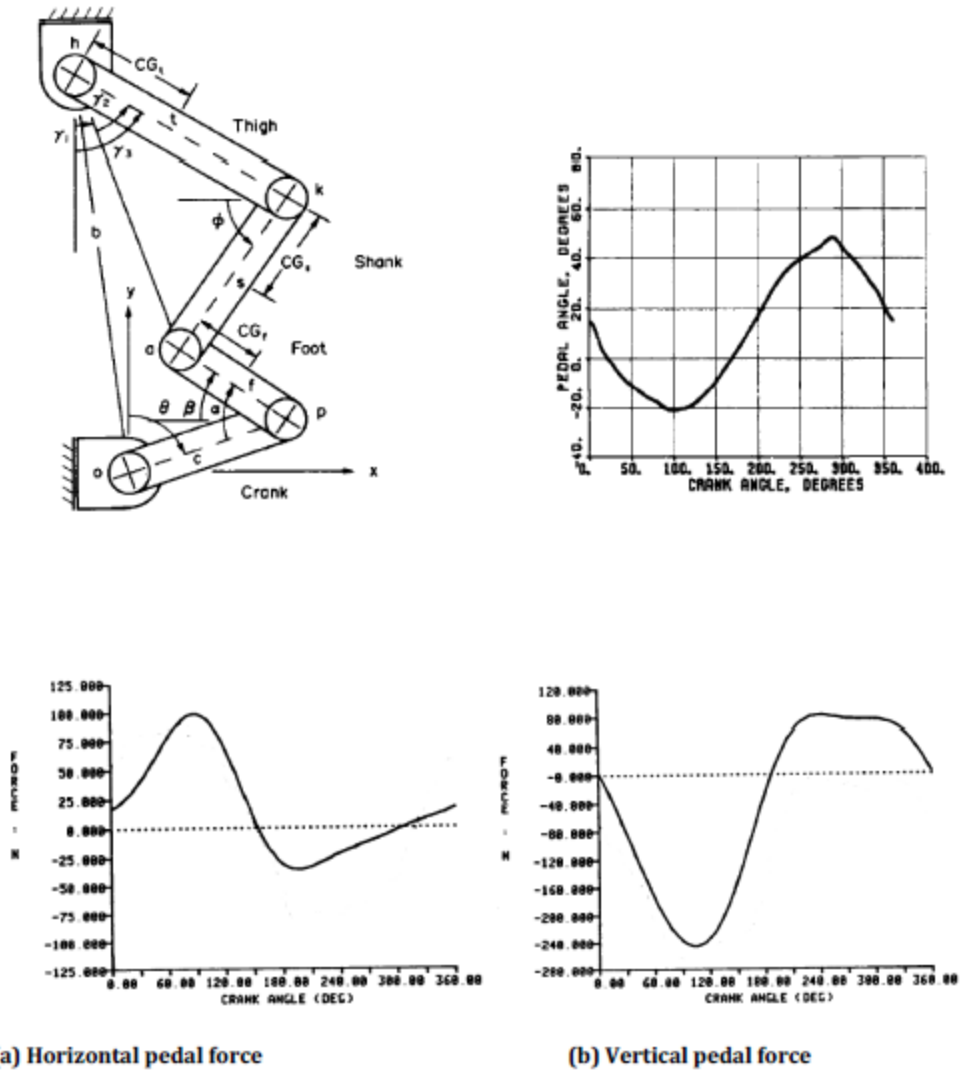


Figure 20: Equivalent mechanical setup, pedal force graphs and angle graphs